Middle-East Journal of Scientific Research 12 (6): 796-800, 2012
ISSN 1990-9233

DOI: 10.5829/idosi.mejsr.2012.12.6.6525

# Earthquakes Relocation in Three-Dimension P-Wave Velocity Model for Abu Dabbab Area, Red Sea, Egypt

*Abu Bakr A. Shater*

National Research Institute of Astronomy and Geophysics, Egypt

**Abstract:** P-wave arrival time data, collected from 150 local earthquakes recorded at 10 telemetered stations located around Abu Dabbab area, has been relocated by three-dimensional velocity model using Simul3 software. Three-dimensional velocity model for earthquake location were computed by inverting the high quality data in the periods from June to August 2004, for hypocenter locations and P-wave seismic velocities. Hypocenters depths ranged from approximately 6 to 12 Km. The present analysis revealed the lateral heterogeneities in the structure of the crust beneath Abu Dabbab area. It was found that the crustal velocity structure at first 1 Km depth is dominated by high velocity zone at the center of the eastern part of the study area and extended down to 12 Km, and low velocity zone appears at the west of the high velocity zone extended down to 12 Km tending to southeast direction. No large systematic shifts of the relocated earthquake locations were observed, except a systematic shift of about 5 km to greater depth. In conclusion, the new relocated earthquake locations showed tighter clustering of epicenters and focal depths when compared with original earthquake locations.

**Key words:** Abu Dabbab Area · Hypocenter Location · Tomographic Inversion · Velocity Model

## INTRODUCTION

Abu Dabbab area is located on the west bank of the Red Sea coast line, to the north of Marsa-Alam city between the longitudes 33.67-35.31°E and the latitudes 24.55-25.65°N, South East of Egypt. It is an active seismic area which Seismic activity is recorded daily and earthquake swarms accompanied by sounds have been known since the beginning of the 20$^{th}$ century [1].

The Abu-Dabbab local telemetered network is consists of 10 short-period seismometers equipped with a vertical seismometer in addition to one Orion station with three components. Data were sent via telemetry to the acquisition center at Marsa-Alam City. It is operated and maintained by the National Research Institute of Astronomy and Geophysics (NRIAG). Figure 1 shows location map and distribution of seismic stations.

Abu-Dabbab Active area was discussed by several authors, like Fairhead and Girdler [2], Daggett *et al*. [3], Hassoup [4], El-Hady [5], Ibrahim and Yokoyama [6].

The accuracy of absolute hypocenter locations is controlled by several factors, including the network geometry, available phases, arrival-time reading accuracy, and knowledge of the crustal structure [7-9]. These factors can be effectively minimized by using joint hypocenter determination method, relative earthquake location methods and tomographic inversion method [10-12].

Thurber *et al*. [13] provided a suitable solution to the problem in order to determine 3-D images of the earth. They proposed a method that uses the a priori velocity model (1-D model), travel times, and hypocentral locations. A good distribution of local earthquakes is required through the area under investigation as well as a good selection of the grid nodes where the a priori model is defined. The grid step depends on the number of rays passing through the model.

**Data:** The data used in this study consisted of 1336 P-Wave arrival times, observed at 10 telemetered stations located around Abu-Dabbab area, from 150 earthquakes occurring beneath the seismic stations during the period from June to August 2004. Figure (4a). The hypocenter location and the origin time of an earthquake were determined by using the HYPO71PC program according to Lee and Lahr [14]. This program needs the P-wave crustal

**Corresponding Author:** Abu Bakr A. Shater, National Research Institute of Astronomy and Geophysics, Egypt.

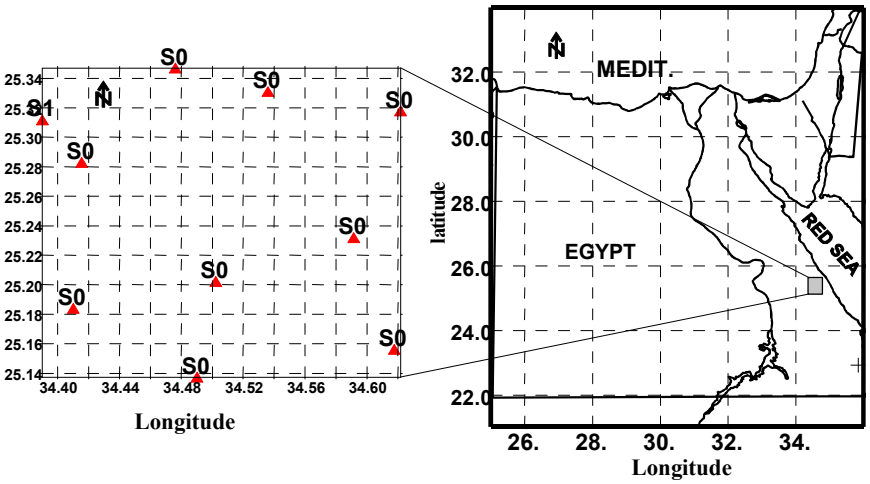


Fig. 1: Location map

Table 1: Seismic stations coordinates

| Station Code | Latitude (deg) | Longitude (deg) | Elevation (meter) |
|---|---|---|---|
| S01 | 25.202 | 34.502 | 550 |
| S02 | 25.346 | 34.617 | 320 |
| S03 | 25.184 | 34.476 | 450 |
| S04 | 25.232 | 34.410 | 520 |
| S05 | 25.137 | 34.592 | 340 |
| S06 | 25.317 | 34.490 | 494 |
| S07 | 25.331 | 34.622 | 285 |
| S08 | 25.283 | 34.536 | 412 |
| S09 | 25.312 | 34.416 | 459 |
| S10 | 25.156 | 34.390 | 507 |

Table 2: P-wave velocity crustal model for the area, used as reference in the 3-D tomography

| Depth (km) | P-wave Velocity (km/s) |
|---|---|
| 0.0 | 4.30 |
| 1.0 | 4.45 |
| 3.0 | 5.90 |
| 9.0 | 6.25 |
| 12.0 | 6.50 |
| 20.0 | 6.80 |
| 25.0 | 7.50 |
| 32.0 | 8.10 |

structure model as shown in table 2. Finally, we choose 150 earthquakes whose depths range from 6-12 km. The initial velocity model is the laterally homogeneous model used for routine hypocentral locations. We use the results of the routine work processing as our initial hypocenteral coordinates and origin times.

## MATERIAL AND METHODS

The computer program Simul 3 third edition written by Thurber [15] was used for solving inversion model parameters and hypocenter locations. The coordinate origin is placed at 25.123 N, 34.390 E. The area was selected as 23 km to the east and 25 km to the north from the origin point (23 by 25 km$^2$). The velocity model is represented by velocity values specified on a three-dimensional grid of nodes (grid point). The nodes are located at the intersection of three sets of planes with normal in the x, y, and z directions. The spacing between any pair of adjacent planes was chosen as 3, 5, 8, 10, 13, 15, 18, 20, 23 and 25 km in x direction (longitude), 3, 6, 8, 11, 13, 17, 18 and 23 km in y direction (latitude) and 1, 3, 9 and 12 km in z direction (depth). The seismic grids should be contained within the seismic array. Velocity values at points within the grids are calculated using a simple interpolation scheme. Given the velocity values at the eight grid points surrounding a certain point (P) within the model. The velocity at (P) is a weighted sum of those eight values. The weights are products of three linear tapers in the X, Y, and Z directions. These weights are also used in apportioning the velocity partial derivatives in the inversion step. Detailed discussions of the inversion method are given by Aki and Lee [16].

The residual time $r_{ij}$ between observed and calculated arrival times at station $i$ from an earthquake $j$, given an initial estimate of hypocenter location and origin can written as:

$$r_{ij} = \sum_{k=1}^{3} \frac{\partial T_{ij}}{\partial Xk} \Delta Xk + \Delta t + \sum_{i=1}^{1} \frac{\partial T_{ij}}{\partial mi} \Delta mi \qquad (1)$$

Whereas $mi$ represent the parameters of the velocity model. The velocity model partial derivatives $\partial T_{ij}/\partial m_i$ are essentially line integrals along the raypath reflecting the relative influence of each model parameters on a given travel time datum.

## RESULTS AND DISCUSSION

Precise earthquake location provides initial insight into observed seismicity and faults or subsurface structures responsible for the observations.

Ibrahim and Yokoyama [6] studied the microearthquake swarm which occurred in 1993 in the Abu-Dabbab area and they concluded that the microearthquake swarms there are not deeper than 16 km and are due to igneous intrusions.

El Hady [5] studied geothermal evolution of the Red Sea margin and its relation to earthquake activity.

Local earthquake tomography is a natural approach to determine reliable three-dimensional velocity models for earthquake locations. Numerous applications of local earthquake tomography to relocate earthquakes exist e.g., Miller and Smith [17], Hauksson [18], Hole *et al*. [19], Husen *et al*. [20], Prantik *et al*. [21], Erdinc and Kennett [22] and Robert *et al*. [23].

The results from a three-dimensional inversion of the local P-wave travel time data without a detailed interpretation, because that is beyond the scope of this study. Following the method in the proceeding section. Fig. 2 shows the cross section of the 2-D P wave velocity structure (A- B for longitude direction and D-C for latitude). At first 1 Km depth is dominated by high velocity zone at the center of the eastern part of the study area and extended down to 12 Km, and low velocity zone

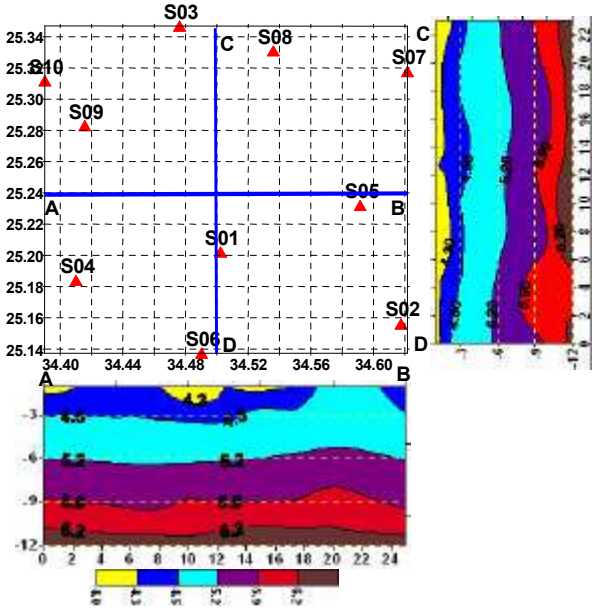


Fig. 2: Cross section of the 2-D velocity structure (A- B for longitude and D-C for latitude)

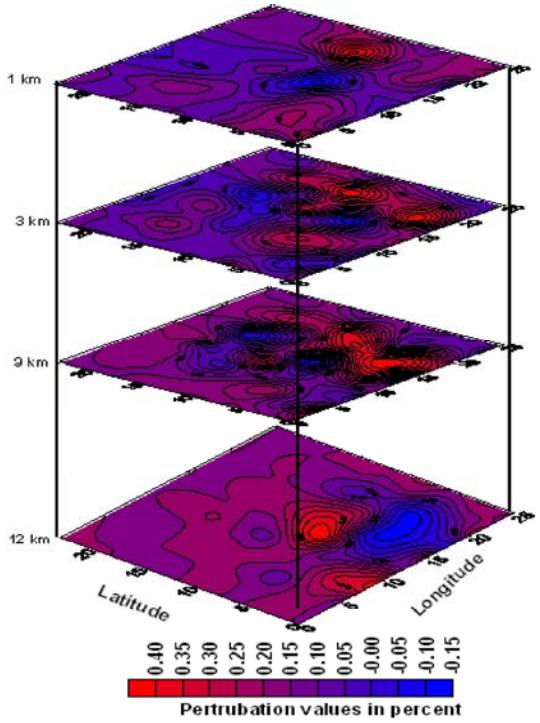


Fig. 3: Final result of the 3-D tomography

appears at the west of the high velocity zone extended down to 9 Km, also high velocity zone appears at south-western part of the area and extended reached down to 3 Km. The overall pattern of velocity perturbation in layer 2 (depth range 1-3 Km) is similar to that of layer 1 except a high velocity zone in the center of the eastern part of the study area is extended horizontally to north and west. Low velocity anomaly in the middle of the target area trending to south-east and north-east starting from depth 3 km and extended down to depth 9 km. Layer 4 is characterized by low velocity zone in the south-eastern side of the target area and sandwiched between two high velocity zones from the north and south-west as shown in Figure 3.

Relocated earthquakes are on average shifts about 0.5 km toward west, 1 km toward north and 5 km deeper than original hypocenter locations (Fig. 4b). Large individual shifts (about 6 km). Relocated focal depths cluster more tightly over a range of 13 km (between 12 km and 14 km depth), whereas original focal depths spread over a range of 8 km (between 6 km and 11 km depth). The other clusters tightly around 15 km depth, whereas original focal depths spread over a range of 10 km (between 6 km and 12 km depth).

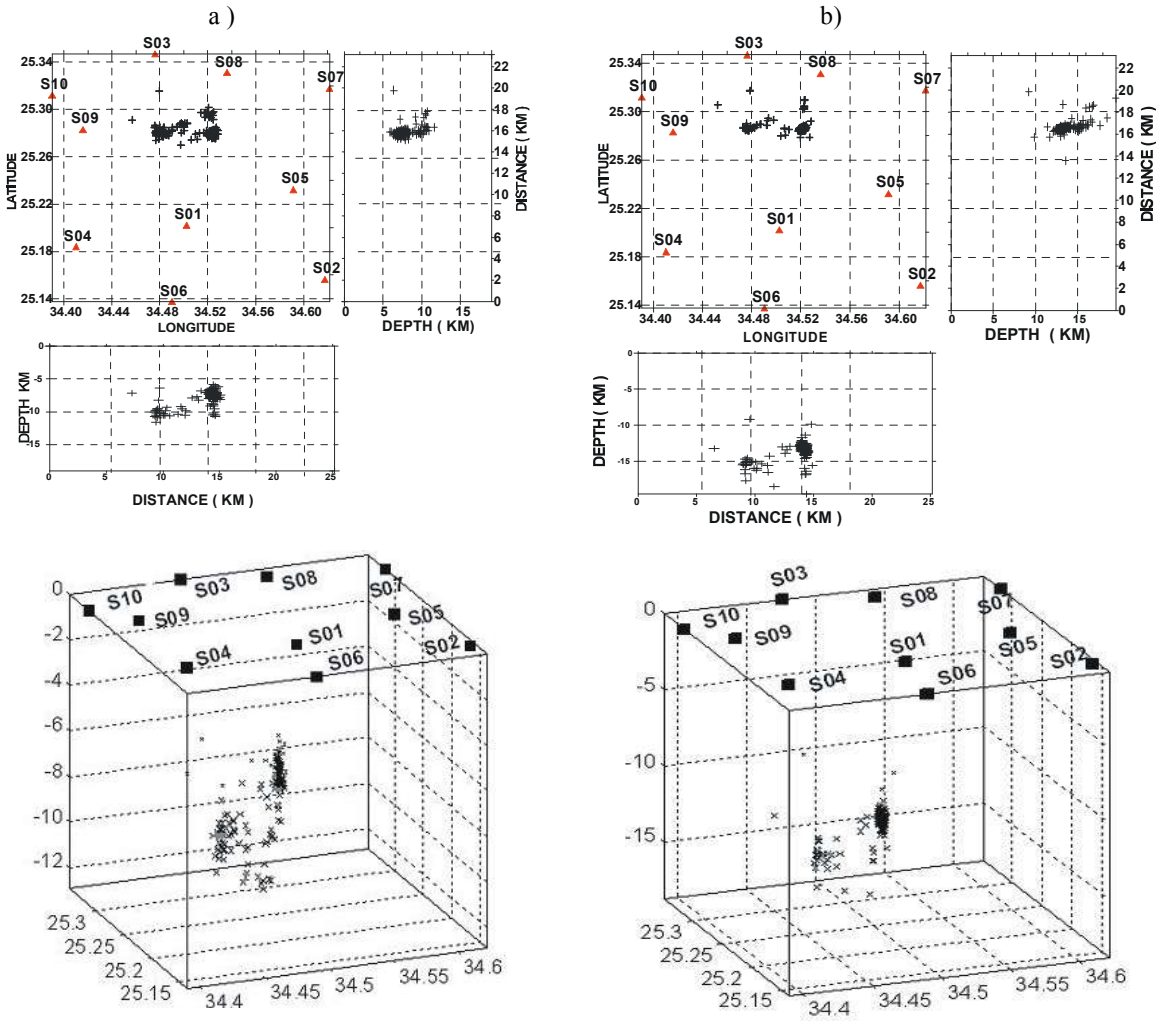


Fig. 4: a) Earthquake Hypocenters b) Relocated hypocenters(map view, cross section and 3-D view)

Figure 4 illustrate the comparison between earthquake hypocenters located using one dimension structure and three- dimension P-wave velocity structure in plane view, cross section and three dimensional views.

The root mean square (RMS) of the weighted pick differential time residuals for the relocated events is 0.017 s, compared to 0.054 s before relocation.

## CONCLUSION

1336 P-Wave arrival times data from Abu-Dabbab seismic network were inverted to compute 3-D velocity model and earthquake relocation. The overall pattern of velocity perturbations were found that the crustal velocity structure at 1 Km depth is dominated by high velocity zone at the center of the eastern part of the area and extended down to 12 Km, and low velocity zone appears at the west of the high velocity zone extended down to 12 Km tending to southeast direction. The relocated earthquakes showed tighter clustering of epicenters when compared with original earthquake locations.

## ACKNOWLEDGEMENT

I would like to express our sincere gratitude and appreciation to Porf. E. M. Ibrahim and Prof. Hesham H. Mousa for their help. I also wish to extend our thanks to all staff of the Egyptian National Seismic Network (ENSN).

## REFERENCES

1. Morgan, P., G.R. Keller and F.K. Boulos, 1981. Earthquake cannons in the Egyptian Eastern Desert. Bull. Seismol. Soc. Am., 71: 551-554.

2. Fairhead, J.D. and R.W. Girdler, 1970. The seismicity of the Red Sea, Gulf of Aden and Afar triangle, Phil. Trans. R. Soc. A., 267: 49-74.
3. Daggett, P.H., P. Morgan, F.K. Boulos, S.F. Hennin, A.A. El-Sherif, A. El- Sayed, A.A. Basta, N.Z. and Y.S. Melek, 1986. Seismicity and active tectonics of the Egyptian Red Sea margin and the northern Red Sea, Tectonophysics, 125: 313-324.
4. Hassoup, A., 1987. Microearthquakes and magnitude studies on earthquake activity at Abu Dabbab region, Eastern Desert Egypt, " Thesis M. Sc., Fac. Sci., Cairo Univ., pp: 1-169.
5. El-Hady Sh, M., 1993. Geothermal evolution of the Red Sea margin and its relation to earthquake activity. M. Sc.Thesis, Cairo University, Cairo, Egypt.
6. Ibrahim, M. E. and I. Yokoyama, 1994. Probable origin of the Abu Dabbab earthquakes swarms in the Eastern Desert of Egypt. Bull. IISEE, 32: 1998.
7. Pavlis, G.L., 1986. Appraising earthquake hypocenter location errors: a complete, practical approach for single-event locations. Bull. Seism. Soc. Am., 76: 1699-1717.
8. Gomberg, J.S., K.M. Shedlock and S.W. Roecker, 1990. The effect of S-wave arrival times on the accuracy of hypocenter estimation. Bull. Seism. Soc. Am., 80: 1605-1628.
9. Waldhauser, F. and W.L. Ellsworth, 2000. A double-difference earthquake location algorithm: Method and application to the northern Hayward fault, Bull. Seismol. Soc. Am., 90: 1353-1368.
10. Poupinet, G., W.L. Ellsworth and J. Fre´chet, 1984. Monitoring velocity variations in the crust using earthquake doublets: An application to the Calaveras Fault, California, J. Geophys. Res., 89: 5719-5731.
11. Hurukawa, N. and M. Imoto, 1987. P and S velocities in the source region of subcrustal earthquakes in the Tokai district, central Japan, J. Phys. Earth, 35: 1-7.
12. Got, J.L., J. Fre´chet and F.W. Klein, 1994. Deep fault plane geometry inferred from multiplet 1relative relocation beneath the south flank of Kilauea, J. Geophys. Res., 99(15); 375-15,386.
13. Thurber, C.H., P.D. Eberhart and J.R. Evans, 1999. Local earthquake tomography: velocity and Vp/Vs-theory, seismic tomography: Theory and practice, pp; 563-583, (H. M. Iyer and Hirahara, K., eds.), Chapman and Hall, London.
14. Lee, W.H.K. and J.C. Lahr, 1972. A computer Program for determining hypocenter, magnitude, and first motion pattern of local earthquakes, U. S. Geol. Survey open file Rep., pp: 75-311.
15. Thurber, C.H., 1985. Simul 3, Third edition, S.U.N.Y. AT; Stony Brook.
16. Aki, K. and W.H. Lee, 1976. Determination of three-dimensional velocity anomalies under a seismic array using first arrival times from local earthquakes 1, A homogeneous initial model, J. Geophys. Res., 81: 4381-4399.
17. Miller, D.S. and R.B. Smith, 1999. P and S velocity structure of the Yellowstone volcanic ?eld from local earthquake and controlled-source tomography, J. Geophys. Res., 104(15): 105-15,121.
18. Hauksson, E., 2000. Crustal structure and seismicity distribution adjacent to the Pacific and North America plate boundary in southern California, J. Geophys. Res. 105(13): 875-13,903.
19. Hole, J.A., T.M. Brocher, S.L. Kelmperer, T. Parsons, H.M. Benz and K.P. Furlong, 2000. Three-dimensional seismic velocity structure of the San Francisco Bay area, J. Geophys. Res. 105(13): 859-13,874.
20. Husen, S., R.B. Smith and G.P. Waite, 2004. Evidence for gas and magmatic sources beneath the Yellowstone volcanic ?eld from seismic tomographic imaging, J. Volcanol. Geotherm. Res., 131: 397-410.
21. Prantik, M., S. Horton and J. Pujo, 2006. Relocation, Vp and Vp/Vs Tomography, Focal Mechanisms and other related studies using aftershock data of the Mw 7.7 Bhuj earthquake of January 26, 2001, J. Ind. Geophys.Union, 10(1): 31-44.
22. Erdinc, S. and B.L.N. Kennett, 2010. Ambient seismic noise tomography of Australian continent Tectonophysics, 481(1–4): 15, 116-125.
23. Robert, D.H., L.V. Frank, V. Martynov, Trilby Cox, E. Jennifer, G.H. Karasu, J. Tylell, L. Astiz and G.L. Pavlis, 2012. Upper Mantle Heterogeneity beneath North America from Traveltime Tomography with Global and USArray Transportable Array Data, Seismological Research Letters, 83: 23-28.